Temperature dependence of serum protein adsorption in PEGylated PNIPAm microgels

Tatiya Trongsatitkul, Bridgette M. Budhlall *

Department of Plastics Engineering and NSF Center for High-Rate Nanomanufacturing, University of Massachusetts, Lowell, MA 01854, United States

ARTICLE INFO

ABSTRACT

The effect of PEGylation on the thermal response and protein adsorption resistance of crosslinked PNIPAm microgels was investigated. It was found that the presence of PEG, its molecular weight (M_n 300 and 1100 g/mol) and its concentration (10, 20, and 30 wt.%) each significantly influenced both the value and breadth of the volume phase transition temperature (VPTT) and the adsorption of bovine serum albumin (BSA) on the surface of the microgels. Specifically, as the degree of PEGylation increased, the value and breadth of the VPTT increased, and the adsorption of BSA decreased significantly. The critical concentration that minimizes protein adsorption on PNIPAm-co-PEGMa microgels was found to be 20 wt.% of PEGMa. This critical concentration was confirmed qualitatively using laser scanning confocal microscopy (LSCM). Evidence for the effect of the molecular weight of PEG on the structure of PNIPAm-co-PEGMa microgels was provided by thermal analysis using differential scanning calorimetry. The VPTT study revealed significant differences in the composition of the microgels when PEGMa samples with two different molecular weights were used as comonomers with PNIPAm. It was determined that the molecular weight and concentration of PEGMa controls the structure of the microgels, which in turn influences their temperature response and protein adsorption resistance properties of the microgels. Our work establishes specific design concepts for controlling the molecular architecture of the hydrogels in order to tune their temperature response and biocompatibility for use in a variety of biomedical applications such as, cell encapsulation, drug delivery and tissue engineering applications.

© 2012 Elsevier B.V. All rights reserved.

1. Introduction

Poly(N-isopropyl acrylamide), PNIPAm microgels are among the most studied *smart* materials as vehicles for drug delivery systems. Hydrated microgels of crosslinked PNIPAm have been shown to exhibit a significant volume change at a temperature of 32 °C, known as the volume phase transition temperature or VPTT [1–3].

At or above VPTT the hydrated microgel collapses and releases the aqueous solution from within. Accordingly, microgel deswelling at VPTT can be used as a mechanism for drug loading and drug delivery. When their VPTT is tailored to be at or above physiological temperature, PNIPAm microgels become especially attractive for biomedical applications.

In order to use PNIPAm microgels as a delivery system, many other factors need to be explored. Biocompatibility of the microgel is one of the most important. The cytotoxicity of PNIPAm has been studied with mixed results. In general, acrylamide-based polymers have been shown to be cytotoxic, leading to activation of platelets on contact with blood [4]. More recent studies [5–8], however,

showed no acute toxicity when PNIPAm was used in eye-drop preparations or as a new embolic material for neurosurgery. To ensure the successful use of PNIPAm-based microgels in biomedical applications, its biocompatibility may need to be improved.

PEGylation is a common technique used to improve the biocompatibility of foreign matter and increase circulation time in the body for proteins, drugs, and drug delivery vehicles [9–16]. PEGylation involves covalently bonding polyethylene glycol (PEG) or polyethylene oxide (PEO) to a species of interest (molecule or particle). PEG and PEO are water-soluble, uncharged, non-toxic, and non-immunogenic polymers [9,10,17–19]. In the body, they form a protective hydration layer on the surface of the species of interest, providing steric hindrance that prevents interaction of proteins with the species. This is known as the "*stealth-effect*". The hydrophilic nature of PEG also minimizes non-specific protein interaction of the PEGylated species, which is believed to play a key role in determining its biocompatibility [20]. We reported previously that PNIPAm-co-PEGMa microcapsules showed significant improvement in the cell viability of encapsulated yeast cells while maintaining their thermoresponsive properties [21].

Recently, Gan and Lyon [18] reported on the effectiveness of PEG modification to decrease protein adsorption on PNIPAm colloidal microgels. PEG-modified PNIPAm core-shell microgels were

synthesized via a two-stage free radical precipitation polymerization using a thermal initiator and a single molecular weight (M_w) of 1000 g/mol PEG. Using the two-stage (seeded polymerization) they attempted to incorporate PEG either within the core or shell of the sub-micron sized microgel particles that were stabilized by anionic surfactants. Unexpectedly, it was found that PEG side chains were able to reduce the adsorption of bovine serum albumin onto PNI-PAm microgels when PEG was incorporated both within the core and the shell. An analysis of the potential competitive adsorption between the surfactant and BSA was not made in order to clarify whether the surfactant could be a contributor to the similar protein adsorption results obtained for the microgels prepared when PEG is localized in either the particle core or shell.

On the contrary, in our study a simple but robust "*microarray technique*" was used to synthesize PNIPAm-*co*-PEGMa microgels that are surfactant free. This is a batch process that facilitates preparation of individual microgels singly or many in an array, each with highly monodispersed particle size and copolymer composition. This technique was designed as a *proof-of-concept* process to control the microgels' structure, composition and particle size. This control facilitated a systematic investigation of the effect of PEGMa molecular weight, concentration, and temperature on protein adsorption on the surface of surfactant-free microgels. Also, in the present study, the protein adsorption was confirmed experimentally using two very different techniques. A direct measurement by visualization of the protein adsorption of fluorescently labeled BSA was made by LSCM and a more quantitative measurement of BSA protein adsorption was made by UV–vis spectrophotometry.

It was expected that the presence of PEG would profoundly alter the properties of the microgels. Specifically, hydrophilic modification of PNIPAm with PEG was expected to decrease its protein adsorption and its hydrophilic–hydrophobic balance, which in-turn would influence its thermoresponsive behavior. To examine the above hypotheses, microgels of PNIPAm and PNIPAm-*co*-PEGMa with varying degrees of PEGylation (0–30 wt.%) were synthesized and compared. PEG macromonomers with number average molecular weights (M_n) of 300 and 1100 g/mol were also compared. Bovine serum albumin (BSA) was used as a model protein in order to investigate the influence of PEGylation on biocompatibility of PNIPAm-based microgels because it is the most abundant serum protein in mammals.

In summary, our study aims to provide a fundamental understanding of the effect of PEG, its concentration, and its molecular weight on properties related to the performance of PNIPAm-*co*-PEGMa microgels in drug delivery applications.

2. Materials and methods

2.1. Materials

All chemicals used in this study were purchased from Sigma–Aldrich (Milwaukee, WI), unless otherwise noted, and were used as-received without further purification. *N*-isopropylacrylamide (NIPAm) and acrylamide (Am) were used as comonomers. *N,N'*-methylenebisacrylamide was used as the crosslinker (MBAm). Polyethylene glycol monomethyl ether monomethacrylate (PEGMa) macromonomer with a M_n of 300 or 1100 g/mol was used as an additional comonomer.

Anthraquinone-2-sulfonic acid sodium salt monohydrate and 2,2-dimethoxy-2-phenylacetophenone were used together as photoinitiators. Low viscosity, high density mineral oil was used as the continuous phase for water-in-oil (w/o) emulsions used to synthesize the microgels. Fluorescein isothiocyanate (FITC) (Fluka) was used to fluorescently label the aqueous phase (containing the monomers) during the microgel synthesis and temperature

response study but not for the protein adsorption study. BSA was used as a model protein in the quantitative protein adsorption study, while FITC-tagged BSA (4 mol dye/mol, Invitrogen) was used in the corresponding qualitative LSCM study. Deionized (DI) water was purified using Millipore Elix 3 system (18 MΩ-cm resistivity) and used in all experiments. Details of the recipe and chemical compositions of PNIPAm-based microgels was given previously [21].

2.2. Synthesis of PNIPAm-based microgels

A microarray technique was used to synthesize the thermoresponsive microgels. A detailed description of this technique has been described elsewhere [21]. This technique allows for real-time observation under a microscope and only requires a small amount of material. It is important to note though, that this technique does not utilize surfactants to stabilize the microgels; therefore it can be considered a surfactant-free process as in the case of Pickering emulsions for example [22]. It is a small-scale batch process, which when scaled-up will require the use of surfactants to stabilize the microgels. Briefly, using PDMS (Sylgard® 184) coated hanging-drop microslides we filled the cavities on the slide with 250 μL of mineral oil. Then, aqueous (1 μL) droplets containing monomer, comonomers, crosslinker, photoinitiators, and fluorescent dye (in all cases but protein adsorption studies) were placed on the surface of mineral oil in each microslide cavity. The photopolymerization was initiated by irradiating with UV light (Sylvania H44GS-100 Mercury Vapor Black Light) positioned 10 cm above the microslide. The polymerization was completed within 30–45 min with the final product a spherical microgel with a diameter of approximately 500 μm that floats on the surface of the mineral oil.

2.3. Effect of PEGylation on volume phase transition temperature

VPTT of PNIPAm-based microgels was studied using laser scanning confocal microscopy (LSCM) and confirmed by differential scanning calorimetry (DSC). The LSCM (Fluoview300, Olympus) equipped with a digital camera (DP7, Olympus) allowed real-time observation of the microgels. Images of PNIPAm-based microgels were acquired at 5 °C increments from 25 to 55 °C. Temperature control during microscope observations was achieved by using a warm-stage (WS50-STC20A, Instec) fixed to the stage of the microscope. The samples were equilibrated at each temperature for at least 5 min before microscope images were acquired. The normalized difference in diameter and the deswelling ratio of the microgels were calculated using Eqs. (1) and (2), respectively.

The particle sizes were determined from the microscope images using NIH *ImageJ* analysis software. The individual particles in the microscope images were detected by applying a segmentation algorithm available within the *ImageJ* program. This algorithm sets the threshold level, where pixel intensities below a set level were assumed to be associated with individual microgels. For each distinct microgel detected, its dimensions were determined by fitting the projected area diameter which is defined as the diameter of a sphere having the same projected area as the microgel. This method was chosen so as to ensure that the circular and non-circular microgels were all measured using a consistent criterion.

The temperature dependent diameter was calculated as follows:

$$D_n = \frac{D_{25\,°C} - D_T}{D_{25\,°C}} \tag{1}$$

$$Q = \frac{D_{25\,°C} - D_{55\,°C}}{D_{25\,°C}} \tag{2}$$

where D_n is the normalized difference in diameter of a sample at temperature (D_T) compared to its initial diameter at 25 °C ($D_{25\,°C}$)

and Q is the normalized deswelling ratio of the difference in diameter of the sample at 55 °C compared ($D_{55\ °C}$) to its initial diameter at 25 °C ($D_{25\ °C}$).

The experiment is conducted at the highest temperature of 55 °C, mainly to ensure that the temperature is greater than the VPTTs of the microgels (highest at ~48 °C for 10 wt.% PNIPAm-*co*-PEGMa M_n 1100 g/mol, as indicated in the DSC result). Even at 55 °C, complete deswelling of thermoresponsive hydrogels may not occur. In fact, it is well known that a significant amount of fluid, (up to 30%) remains in PNIPAm gels at temperatures above the VPTT of the hydrogel [23]. Since 45 °C is the human pain threshold [24], it is advisable to not employ thermal therapies in the body that exceed that temperature. As such, using 55 °C as the maximum testing temperature is appropriate to understand the temperature responsive property of the microgels above VPTT. No additional useful information for the drug application will be obtained if the test is performed above 55 °C.

DSC (Q200, TA Instruments) was used to determine the VPTT of PNIPAm and PNIPAm-*co*-PEGMa copolymers. The microgels were prepared via the microarray technique and were first rinsed with DI water to remove the mineral oil from their surface. They were then soaked in DI water for 24 h to ensure they were fully hydrated. These fully hydrated microgels were then tested against DI water which was used as the reference. A scanning rate of 5 °C/min under nitrogen gas purge was employed. The second heating of the *heat–cool–heat* cycle was used to analyze the calorimetric data (via TA Universal Analysis software) in order to determine the VPTT and melting transition (T_m).

2.4. Effect of PEGylation on serum protein adsorption

Two protein adsorption experiments were performed. First, a qualitative protein adsorption study was performed via LSCM. The purpose of this experiment was to directly observe the protein adsorption onto the microgels' surface using FITC-tagged BSA. The microgels were synthesized using the previously described microarray technique except that the FITC dye was not used [21,25]. Three microgels were incubated in FITC-tagged BSA protein solution (1.0 wt.% in 0.1 M phosphate buffered saline [PBS]) at room temperature for 24 h to achieve saturation in adsorption. The samples were then separated from the protein solution and quickly rinsed with DI water before observations under LSCM. Using LSCM with an excitation wavelength (λ_{ex}) of 495 nm and emission wavelength (λ_{em}) of 518 nm, only FITC-tagged BSA protein can be seen. Therefore, this experiment revealed coverage of PEG on the surface of the microgels assuming that protein adsorbs on PNIPAm but not on PEG.

In addition, it is expected that there will be some absorbance of BSA onto the quartz cuvette and glass vials that held the samples via ionic amine–silanol bonding and hydrogen bonding. It was assumed however, that the amount of protein adsorbed on the cuvette or glass is the same in all samples and the results obtained should be considered normalized. The differences shown for each sample are the result of 30 different microgels. The results were reproducible and repeatable.

Second, a quantitative protein adsorption study was conducted using UV–vis spectrophotometry. The intrinsic absorbance of aromatic amino acids in BSA at 280 nm was measured using a UV–vis spectrophotometer (Lambda 1806) [26]. Various concentrations of BSA solutions were prepared in 0.1 M PBS buffer to establish a standard curve (see Fig. S1 in Supporting Information). With the standard curve, a linear relationship between UV absorbance intensity and BSA concentration indicates that Beer–Lambert's law can be applied to determine the concentration of an unknown protein solution. An optimization experiment was performed to determine the BSA concentrations that fell within the linear dependence

of absorbance on concentration as delineated by Beer–Lambert's law. Typically the rule of thumb is to use concentrations that give absorbance in the range 0.5–1.0. In the present study, 30 microgels at a concentration of 0.07 mg/mL gave BSA absorbance within this range. Consequently, the effect of PEGylation on the protein adsorption was examined by introducing thirty microgels of each sample into 4 mL of 0.07 mg/mL BSA in 0.1 M PBS solution.

The mixtures were incubated as before, by standing at 25 and 37 °C for 24 h to achieve saturation in adsorption. It was verified in a control experiment that 24 h is sufficient to reach equilibrium in adsorption (see Fig. S3 in Supporting Information). The supernatant was then extracted, and by using Beer–Lambert's law, the concentration of BSA protein remaining in the supernatant was determined. The concentration of BSA protein adsorbed on the microgels was then calculated from the difference in the concentrations before and after incubation. Three replicates of each microgel were performed and are presented as an average value ±1 standard deviation.

3. Results and discussion

3.1. Effect of PEGylation on PNIPAm-based microgel morphology

It has been shown [27–29] that the cross-linker distribution within PNIPAm microgels particles is in general, heterogeneous. It was explained by McPhee et al. [30] that the cross-link density decreases from the center to the periphery because of the difference in reactivity ratios of the comonomers. They have shown that the reactivity of MBAm is greater early on in the synthesis and hence the cross-linker is consumed at a faster rate, earlier than NIPAm, resulting in a higher crosslinked core. In addition, the reactivity ratios of NIPAm and PEGMa reported by Alava et al. [31] are r_{NIPAm} = 1.2 and r_{PEGMa} = 0.13, respectively which indicates that NIPAm prefers to react to its own species and PEGMa prefers to react to another species rather than itself. From this information we can safely hypothesize that the general microgel architecture is as shown in Fig. 1.

This morphology in principle is also supported by the miscibility of the comonomers and their corresponding polymers' expected phase separation after polymerization due to the migration by diffusion of the more hydrophilic PEG to the outer surface leaving the less hydrophilic (relatively) PNIPAm toward the inner shell and core. This hypothesis was tested by elucidating the effect of M_w and concentration of PEG in the microgels on its temperature response, VPTT and protein adsorption the results of which are presented in the next section.

3.2. Effect of PEGylation on temperature response and volume phase transition temperature of PNIPAm-based microgels via LSCM

The VPTT of PNIPAm can be increased by copolymerization with hydrophilic comonomers. In the current study, PNIPAm-*co*-Am (hence-forth referred to as PNIPAm microgels for simplicity) possess a VPTT in the range of 32–35 °C. By incorporating another hydrophilic monomer – PEGMa, it is expected that the VPTT would be further increased to between 38 and 45 °C.

The temperature response of PNIPAm microgels over the temperature range of 25–45 °C is illustrated in Fig. 2. The confocal images show the PNIPAm microgel decrease in size as the temperature is increased. Quantitative measurements of the microgel shrinkage were conducted by determining its diameter at different temperatures and then normalizing this to its initial diameter measured at 25 °C. The comparison of the normalized difference in diameter of PNIPAm-based microgel and its copolymers
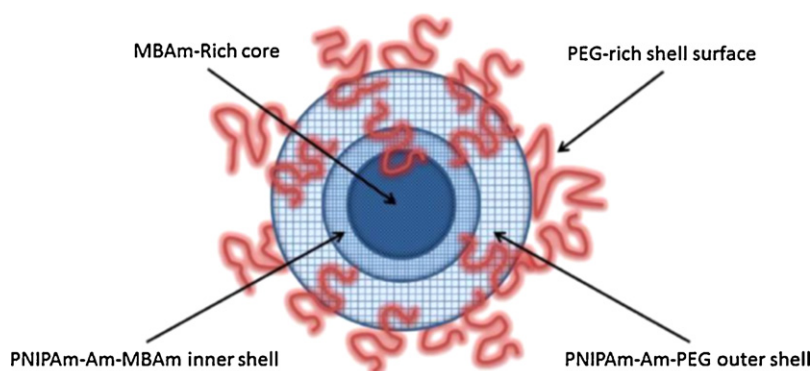
Fig. 1. Illustration of hypothesized structure of PEGylated PNIPAm microgel based on the reactivity ratios of the comonomers used in the system.
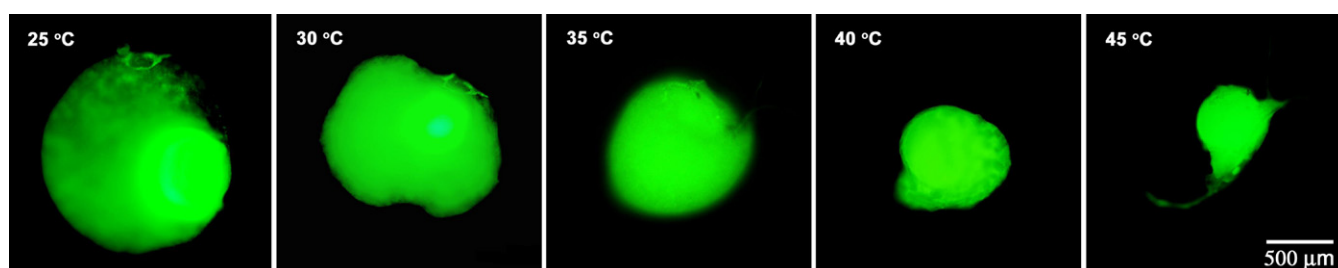

Fig. 2. LCSM micrographs of PNIPAm microgel showing deswelling as the temperature is increased. FITC is used to fluorescently label (green fluoresence) the polymer in the LSCM study only.

PNIPAm-*co*-PEGMa is shown in Fig. 3. A higher normalized difference in diameter indicates a larger decrease in diameter. A sharp slope over a range of temperatures indicates a significant change in diameter or the VPTT of the microgel. The plot of the normalized difference in diameter of PNIPAm microgel in Fig. 3(a) exhibits the maximum change in slope as the temperature is increased from 30 to 35 °C. This indicates that the maximum deswelling of PNIPAm microgel occurred within this temperature range. The latter temperature falls within the typical lower critical solution temperature or LCST for PNIPAm.

To investigate the effect of chain length on the overall phase transition temperature and the temperature response behavior of the microgels, PNIPAm was copolymerized with PEGMa with two different molecular weights (M_n 300 and 1100 g/mol).

The temperature response results for PNIPAm and PNIPAm copolymerized with a low molecular weight PEGMa (M_n 300 g/mol) at different concentrations (10, 20, and 30 wt.%) are shown in Fig. 3(a). The presence of PEGMa in the PNIPAm microgel caused the deswelling to occur at higher temperatures and over a broader temperature range compared to that of PNIPAm microgel alone. This result is similar to that observed previously [18,19,32–36]. The widening and increase of VPTT is due to the greater hydrophilic nature of PEG compared to PNIPAm, which results in shifting of the hydrophilic/hydrophobic balance of the microgel. This change in temperature response behavior implies that the PEGylated PNI-PAm microgel is less temperature responsive and its response is less defined as compared to the PNIPAm microgel without PEG. This effect becomes more pronounced as the PEGMa concentration in the microgel is increased.

A broadening and increase in VPTT was also obtained when a higher molecular weight of PEGMa (M_n 1100 g/mol) was used (Fig. 3(b)). At the highest concentration tested (30 wt.% PEGMa), two distinct deswelling events occurred. The first occurred when the temperature was increased from 30 to 35 °C and the second when the temperature was increased from 45 to 55 °C. The result suggests that these two transitions belong to VPTT

of PNIPAm (homopolymer) and PNIPAm-*co*-PEGMa (copolymers), respectively. The presence of long chains of PEGMa (1100 g/mol) may enhance their phase separation from PNIPAm during polymerization, therefore the characteristic VPTT of PNIPAm was observed. This hypothesis was tested by DSC and is discussed in the following section.

For both molecular weights, the microgels became less temperature responsive with increasing concentration of PEGMa as indicated by a shallower slope (Fig. 3). At the highest concentration (30 wt.%), a dramatic reduction was seen in the temperature response as indicated by little or no change in the size of the microgel.

3.3. Effect of PEGylation on the volume phase transition temperature of PNIPAm-based microgels via DSC

3.3.1. Low molecular weight PEGMa M_n 300 g/mol

The effect of PEGylation on the transition temperature of PNIPAm-based microgels was further analyzed using DSC. It has been reported in the literature that PNIPAm homopolymer crosslinked with MBAm, has a VPTT of 32 °C in the aqueous phase [1–3]. As shown in Fig. 4, a single endothermic peak corresponding to the VPTT for the PNIPAm copolymerized with Am and crosslinked with MBAm, was found at ∼34 °C. PEGMa (M_n 300 g/mol) microgel, however, does not possess any transition temperature in the testing range. The lack of the melting endotherm in the latter indicates that no long blocks of PEGMa polymer chains are formed. In addition, no melting transition was found in the copolymers prepared with this lower M_n 300 g/mol PEGMa as well. Instead, the single endothermic transition found at all PEGMa concentrations is attributed to the VPTT of the PNIPAm-*co*-PEGMa copolymer. This VPTT increased to 43–44 °C and its width and height increased with increasing PEGMa concentration as compared to that of the PNIPAm-based microgel without PEGMa.

These results implied that a greater amount of energy is required for the volume phase transition to take place. In other words, the
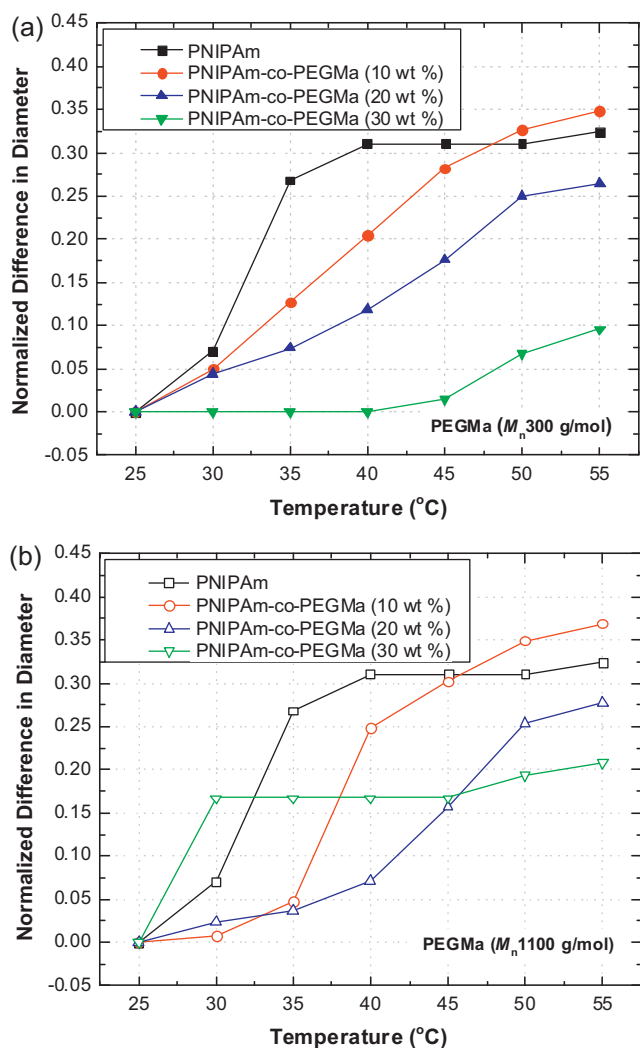
Fig. 3. Effect of PEGylation on the temperature response of PNIPAm-*co*-PEG microgels with two different molecular weights (a) PEG M_n 300 g/mol (solid symbols) and (b) PEG M_n 1100 g/mol (open symbols), at increasing PEG concentrations; 0 wt.% (□), 10 wt.% (○), 20 wt.% (△), and 30 wt.% (▽). The error bar is omitted as the standard deviation is within the size of the symbol. Each data point represents an average value of at least three replicates.

microgels containing PNIPAm-*co*-PEGMa copolymer became less responsive to thermal stimuli as compared to the PNIPAm-based microgels prepared without PEGMa. These results also agree well with our temperature response study using LSCM discussed earlier. In principle, a single endothermic peak corresponding to the VPTT along with its shift to higher temperature indicates that a random copolymer of PNIPAm and PEGMa was formed in this case.

3.3.2. High molecular weight PEGMa M_n 1100 g/mol

The DSC thermographs of the microgels prepared with PNIPAm-*co*-PEGMa (M_n 1100 g/mol) copolymer lacked the melting point of PEGMa at 36 °C but, revealed two endothermic peaks, one at ∼32 °C and the other ranging from 45.9 to 48.1 °C. The disappearance of the melting transition indicated that all of the PEGMa copolymerized with PNIPAm. The first endothermic peak is attributed to the VPTT at ∼32 °C characteristic of crosslinked PNIPAm homopolymer, implying that long chains (or blocks) of PNIPAm-MBAm were formed as a part of the copolymer. This result provides evidence for our hypothesized microgel structure depicted in Fig. 1. The second endothermic peak is attributed to the VPTT of the PNIPAm-*co*-PEGMa (M_n 1100 g/mol) copolymer ranging from 45.9 to 48.1 °C

as the concentration of PEGMa is decreased. Interestingly at low concentrations of PEGMa, the two endothermic peaks are rather weak as compared to the VPTT of PNIPAm or the melting transition of PEGMa alone.

Consider that free-radical polymerization mechanisms typically give a random copolymer as a final product; a random copolymer should be expected when both PEGMa molecular weights (M_n 300 and 1100 g/mol) are copolymerized with NIPAm.

Overall, these findings suggests that the lower M_n 300 g/mol PEGMa with greater mobility and more water-solubility, copolymerizes readily into the growing PNIPAm chain giving a single endothermic VPTT. Whilst, the bulky and less water-soluble higher M_n 1100 g/mol PEGMa may copolymerize with PNIPAm at a slower polymerization rate forming less crosslinked copolymer.

It was also observed that the melting transition of PEGMa M_n 1100 g/mol disappeared when copolymerized. This may be because the smaller NIPAm monomer hinders recrystallization of the PEGMa polymer chains in the copolymers.

The shift in VPTT as measured by DSC is less pronounced than observed in the LSCM studies as seen from Figs. 4 and 3, respectively. That is, from the LCSM measurement on PNIPAm-*co*-PEGMa (30 wt.%, 300 g/mol) a VPTT around 50 °C would be deduced, while the corresponding DSC value is below 45 °C. A plausible explanation for this observation is that the LSCM is not as accurate as the DSC to determine the endothermic VPTT. In the LSCM a study, the temperature was increased in 5 °C increments compared to the more continuous increase performed using the DSC. Therefore, the LSCM results at best estimates the range of temperature over which a significant deswelling occurs.

In summary, a comprehensive analysis of the thermal response revealed by LSCM and DSC provides detailed information about the structure and thermoresponsive properties of the microgels. We found that incorporating PEGMa in the copolymers increased the VPTT and decreased the thermal responsiveness, of the PNIPAm-based microgels. In addition, the value and number of endotherms indicates whether the microgel is composed of a single polymer or a copolymer.

3.4. Effect of PEGylation on thermal reversibility

The normalized deswelling ratio, Q gives the *degree of shrinkage* of the microgel in response to increasing the temperature from 25 to 55 °C. The experimental results of cyclic dwelling-swelling of PNIPAm-based microgels with and without 30 wt.% PEGMa M_n 300 g/mol are shown in Fig. 5, following alternating *heating–cooling* cycles, (where n represents one cycle) between 25 and 55 °C. The thermal cycles, n are repeated more than five times and show that the temperature response is reversible and reproducible. This is indicative of almost 100% water recovery of each microgel, regardless of whether or not PEGMa is present. The extent of shrinkage of PNIPAm was greater than that of PNIPAm-*co*-PEGMa. Therefore, the presence of PEGMa hampers the temperature sensitivity but clearly does not hinder the repeatability of the temperature response for PNIPAm-based microgels. This reversibility plays a critical role in some applications such as drug delivery, which uses swelling and deswelling as a mechanism to load and release therapeutic agents.

3.5. BSA protein adsorption onto PNIPAm-based microgels

Protein adsorption on a surface of materials used in biomedical applications is an important mechanism used by our body to detect and remove foreign objects. Nonspecific interactions of the protein on hydrophobic surfaces play an important role in this process. PNIPAm possesses hydrophobic isopropyl domains that may induce nonspecific interaction with proteins. Copolymerization of PNIPAm with PEGMa improves the biocompatibility of the microgel
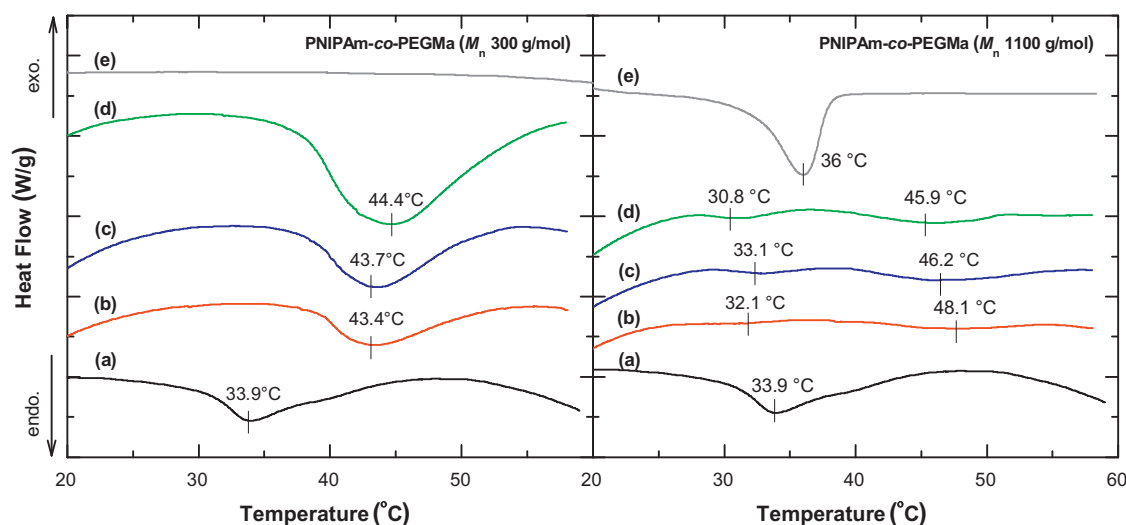
Fig. 4. DSC thermographs of PNIPAm-based microgels copolymerized with three concentrations of two different molecular weights of PEGMa macromonomers. The left and right panels are for PEGMa (M_n 300 g/mol) and PEGMa (M_n 1100 g/mol), respectively, where (a) PNIPAm, (b) PNIPAm-*co*-PEGMa (10 wt.%), (c) PNIPAm-*co*-PEGMa (20 wt.%), (d) PNIPAm-*co*-PEGMa (30 wt.%), and (e) PEGMa (100%). The plots are offset for clarity of presentation and only the second heating in the *heat/cool/heat cycle* is shown, with a heating rate of 5 °C/min.

by preventing the non-specific interactions with proteins. PEGMa is believed to migrate to the aqueous interface, rendering protein adsorption resistance at the surface [18,37].

The internal pore size distribution of PNIPAm-based hydrogels has been found to be between 60 and 100 nm in size [38–40] however, these pores are not continuous and will provide a torturous path for any penetrant. Therefore, since the corresponding calculated volume of the hydrodynamically equivalent sphere [41] of the BSA molecule is 163 nm³, it is reasonable to expect some absorption into the pores. FITC-labeled BSA will have an even larger size than bare BSA. It is assumed however, because of the non-continuous porosity of the gel network the amount absorbed compared to that adsorbed onto the surface of the microgel will be insignificant.

3.5.1. Effect of PEG concentration and molecular weight on BSA adsorption

In these experiments the concentration and molecular weight of PEG were systematically varied and their effects on the resulting
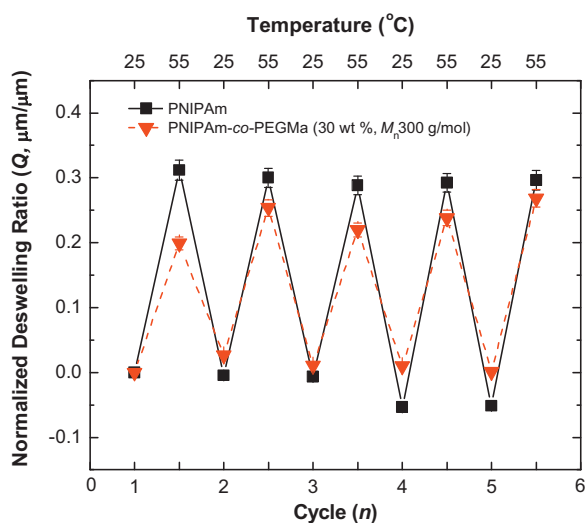

Fig. 5. Normalized deswelling ratio as a function of the number of heating–cooling cycles, *n*, between 25 and 55 °C for PNIPAm (■) and PNIPAm-*co*-PEGMa (30 wt.%, M_n 300 g/mol) (▼). Each data point is an average value of at least three replicates and the error bars show the standard deviation.

PNIPAm-based microgels were investigated. It was expected that PEGylation would provide the required hydrophilic surface modification for the PNIPAm-based microgels to minimize protein adsorption and maximize biocompatibility.

The protein adsorption was observed qualitatively using LSCM. Fluorescent images of PNIPAm microgels after incubation with FITC-tagged BSA showed a significant protein adsorption on their surface (Fig. 6). Under the confocal microscope, a brighter fluorescent green color indicates a higher protein adsorption on the microgel.

The presence of PEGMa induced a reduction in FITC-tagged BSA adsorbed on the microgel surfaces, as seen in Fig. 7. The intensity of FITC-tagged BSA decreased significantly as the PEGMa content increased to 20 and 30 wt.%. The microgels prepared with lower molecular weight PEGMa (300 g/mol) showed a slightly better protein resistance than those prepared with the higher molecular weight PEGMa (1100 g/mol). It is speculated that this is due to a higher number of short PEGMa chains providing a better surface coverage than the lower number of long chains. Evidence that long chains of PEGMa form a loose coil configuration in a good solvent e.g., water [42] suggest that higher molecular weight PEGMa is less effective in preventing protein adsorption.

Quantitative measurements of protein adsorption on PNIPAm-based microgels agree with the qualitative LSCM study discussed previously. From Fig. 8, it can be seen that 20 wt.% PEG is a critical concentration for minimizing protein adsorption on the copolymer. As the concentration of PEGMa is increased beyond 10 wt.%, there is little difference in protein adsorption. These results provide evidence for PEG phase separation during the polymerization to give a microgel architecture as depicted in Fig. 1. It fact, this phase separation is expected after polymerization due to the migration by diffusion of the more hydrophilic PEG to the outer surface leaving the relatively less hydrophilic PNIPAm toward the inner shell and core.

Also shown in Fig. 8, the amount of BSA protein absorbed on PNIPAm microgels in the swollen state (25 °C) is 7 mg BSA/mg microgel, which is about three times greater than that of PEG-based microgels. Incorporating PEG macromonomers (both M_n 300 and 1100 g/mol) into PNIPAm microgels led to a decrease in the degree of BSA absorption on the microgel particles. Interestingly, the protein adsorption decreased drastically when PEGMa at 20 wt.% or greater was used. At these higher concentrations, the amount of
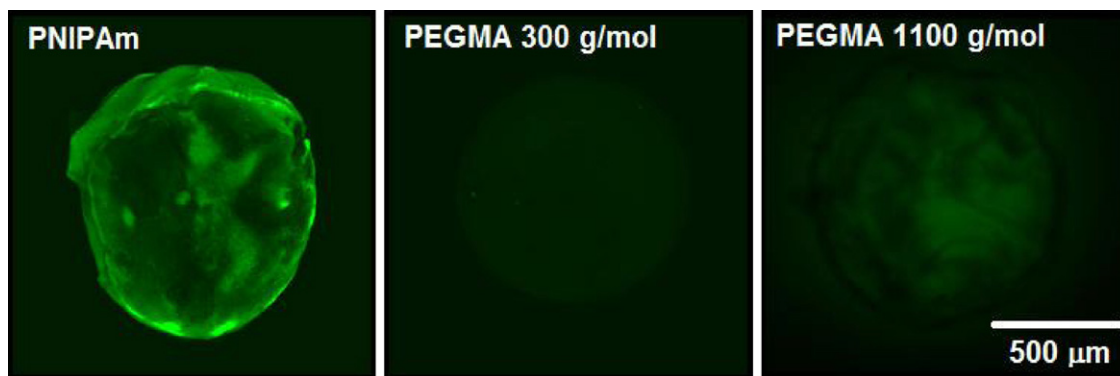
Fig. 6. Fluorescent images of microgels prepared using (a) PNIPAm, (b) PEGMa Mn 300 g/mol, and (c) PEGMa Mn 1100 g/mol after incubation in FITC-tagged BSA solution at 25 °C for 24 h. Note in the protein adsorption study no FITC is added to the polymer, therefore the fluorescent green color is only due to FITC-tagged BSA protein adsorption onto the surface of the microgels.
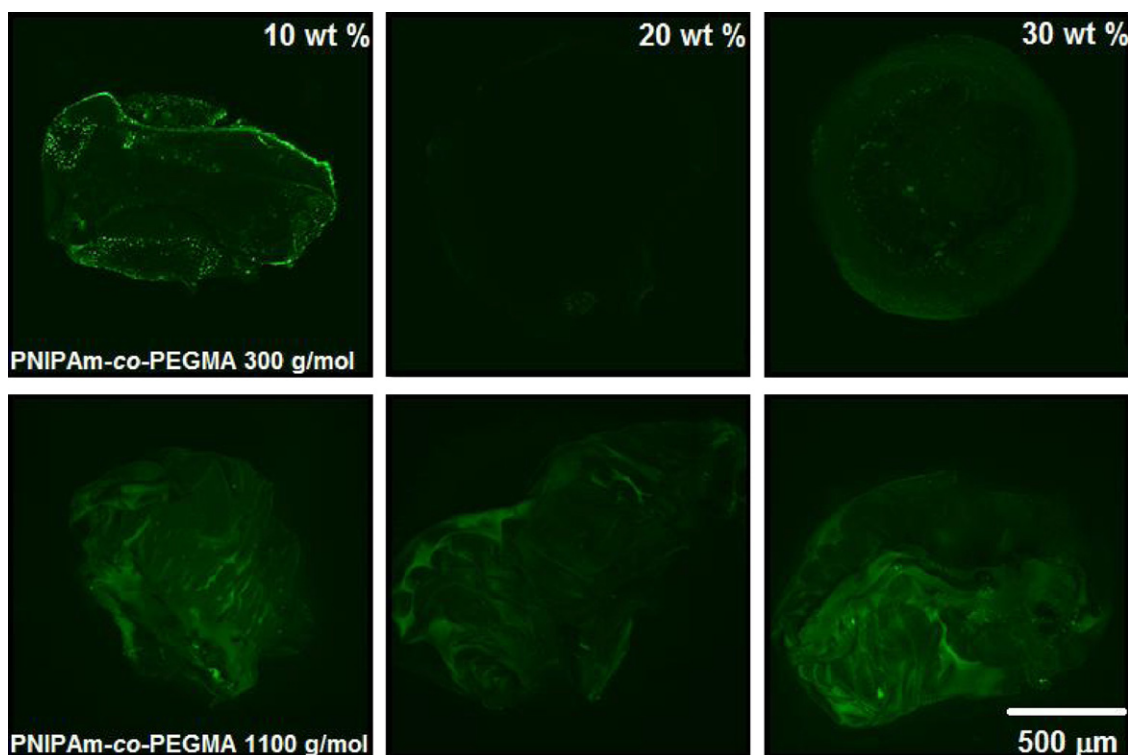

Fig. 7. Fluorescent images of PNIPAm-based microgels comprised of 10, 20, and 30 wt.% PEGMa respectively, with the top row showing PEGMa M_n 300 g/mol and the bottom row showing PEGMa M_n 1100 g/mol. The brighter color indicates higher FITC-tagged BSA protein adsorption in the surface of the microgels and denotes regions rich in PNIPAm (and conversely the dark area denotes regions rich in PEGMa).

the adsorbed protein on the PNIPAm-*co*-PEGMa microgels is in fact close to that adsorbed on the PEG-only microgels.

A possible explanation is that at 20 wt.%, the number of PEG chains is sufficient to cover the entire surface of the microgel particle, as illustrated schematically in Fig. 9. It is speculated that a PEG concentration lower than 20 wt.% can only partially cover the PNIPAm microgel surface. Part of the PEGMa content is believed to be entrapped inside the particle. This hypothesis was confirmed by the observation that a relatively high amount of protein (∼7 mg BSA/mg microgel) was adsorbed on the PNIPAm-based microgels copolymerized with 10 wt.% PEG M_n 300 g/mol. When the longer PEGMa (M_n 1100 g/mol) was used at the same concentration, an observable decrease in protein adsorption (∼5 mg BSA/mg microgel) was obtained. This result implies that the longer PEG chains can protrude and maintain a higher degree of hydration, and hence provide better surface coverage at low PEG content.

The effect of the molecular weight was insignificant and thus negated when the PEGMa concentration was increased above 20 wt.%, however.

3.5.2. Effect of temperature on BSA adsorption

Because temperature affects protein structure, solubility and diffusion rates (to the interface), we also studied the effect of temperature on the protein adsorption. Isolated BSA is reported to partially unfold between 40 and 50 °C, exposing non-polar residues on the surface and facilitating reversible protein–protein interactions [43]. Therefore, at 37 °C, we expect the BSA protein to act normally, and any differences in protein adsorption will be due to the change in surface properties of our microgel, going from a hydrophilic polymer "*coil*" to a more hydrophobic "*globule*" above VPTT. Indeed, increasing the temperature resulted in an increase in BSA adsorption as shown in Fig. 10.
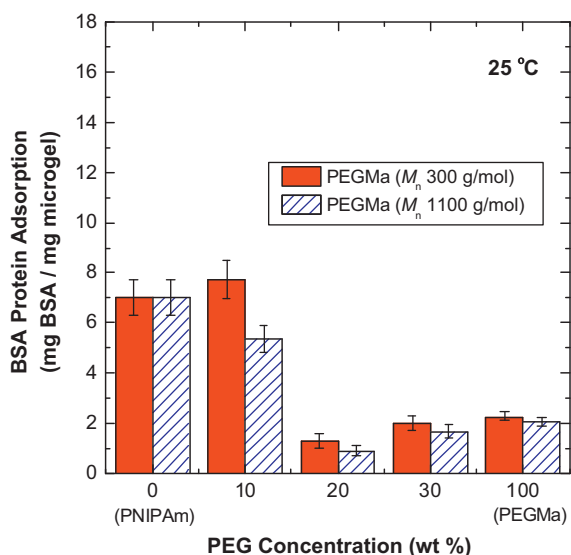
Fig. 8. Protein adsorption (FITC-BSA) results for PNIPAm-based microgels with varying degrees of PEGylation of PNIPAm-co-PEGMa, after incubating at room temperature (25 °C) for 24 h. 0 wt.% denotes the positive experimental control using PNIPAm without PEGMa, and 100 wt.% denotes the negative experimental control using only PEG. Each data point represents an average value of at least three replicates and the error bars show the standard deviations.

Fig. 10. Protein adsorption (FITC-BSA) results for PNIPAm-based microgels with varying degrees of PEGylation of PNIPAm-co-PEGMa, after incubating at 37 °C for 24 h. 0 wt.% denotes the positive experimental control using PNIPAm without PEGMa, and 100 wt.% denotes the negative experimental control using only PEGMa. Each data point represents an average value of at least three replicates and the error bars show the standard deviations.

We hypothesized that this increase is due greater hydrophobic interactions with the hydrophobic polymer surfaces above VPTT. We tested this hypothesis by conducting a control experiment using poly(styrene) (PS) latex instead of the PNIPAm-based microgel. PS is not a temperature responsive polymer and will not exhibit a temperature dependent shrinkage or change in hydrophobicity. Indeed, no change in BSA adsorption of 23 ± 2 mg BSA/mg PS particle is observed with an increase in temperature (from 25 to 37 °C). Hence, in the PNIPAm-based microgels, the increase in protein adsorption at a higher temperature is due to the change in surface properties of the microgel above VPTT. Also, because the protein adsorption is calculated in terms of mg BSA/mg of microgel, this increase in protein adsorption is real and not an artifact of the temperature dependent shrinkage (leading to lower surface area) of the microgel.

These findings support the earlier qualitative LSCM experiments and suggest that the structure of these deswollen microgels above VPTT, containing the higher PEG M_n 1100 g/mol possess long chains that are either mobile enough to protrude from the hydrophobically collapsed network or are enriched at the surface due to phase separation during polymerization as shown schematically in Fig. 9 and noted by Gan et al. [18].
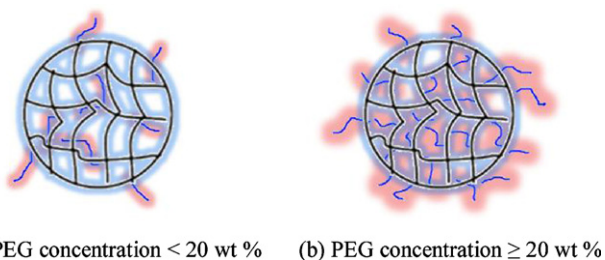

(a) PEG concentration < 20 wt %   (b) PEG concentration ≥ 20 wt %

Fig. 9. Illustration of the surface coverage of PEG chains on PNIPAm-based microgels as a function of degree of PEGylation. (a) At PEGMa concentrations of less than 20 wt.%, the chains partially cover the surface of PNIPAm-based microgel and allowed protein adsorption to occur on the particle surface and (b) conversely, at PEGMa concentrations of 20 wt.% or greater, the chains cover the entire microgel surface, thus preventing protein adsorption.
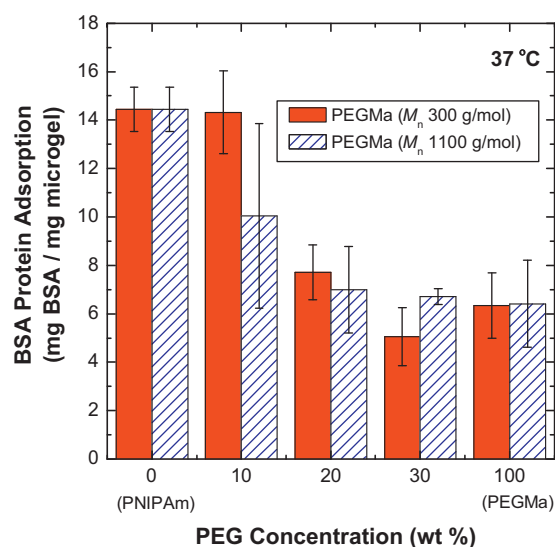
The protein resistance of oligo(ethylene glycol)-terminated self-assembled monolayers (OEG-terminated SAMs), that is, complete reversibility of adsorption, was first reported in the seminal paper by Prime and Whitesides [44], and it was suggested that protein resistance is of entropic origin. Extensive and detailed analysis of the packing density and molecular conformation in OEG-terminated SAMs, measured on dry films, led to the conclusion that because of the conformational constraints imposed by dense packing, an entropic mechanism of protein resistance is unlikely [45]. The importance of water penetration into the OEG terminus of the films to render them protein-resistant was established only later. The penetration of water into OEG-terminated SAMs was recently demonstrated independently by polarization modulation infrared reflection-absorption spectroscopy, PM-IRRAS [46]. In a similar fashion, PEG is expected to decrease its protein adsorption resistance as a function of temperature. The breakdown of the protein resistance of PEG as was observed with OEG-terminated SAMs as a function of temperature *ex situ* with PMIRRAS was not seen, however, in our measurements.

In summary, even though our experimental conditions have not been optimized for surface coverage and PEG chain length; we show here a promising means to achieve temperature responsive PNIPAm microgels with tunable protein adsorption simply by modifying the degree of PEGylation.

4. Conclusions

PEGylation of PNIPAm microgel leads to an increase and broadening of the VPTT of microgels. This is caused by the increased hydrophilicity of the microgels, leading to a lower propensity of PNIPAm to collapse. The introduction of PEGMa into PNIPAm microgels improved their biocompatibility. It was found that 20 wt.% PEGMa is the critical concentration that minimizes BSA protein adsorption on the PNIPAm-co-PEGMa microgels. In addition, when the low molecular M_n 300 g/mol PEGMa is incorporated into the PNIPAm-co-PEGMa copolymer, a more defined VPTT and lower protein adsorption was obtained compared to the high molecular weight PEGMa M_n 1100 g/mol. The increase in hydrophilicity rendered to the microgels by PEGMa also altered the temperature

responsiveness of the microgels. The temperature responsiveness of the PNIPAm-*co*-PEGMa microgels was significantly decreased as compared to microgels prepared using PNIPAm without PEGMa.

The authors believe it is entirely possible to optimize the properties of the microgels to obtain a reasonable deswelling ratio and sufficiently suppress non-specific protein adsorption. In fact, the practical consequence of our findings is that in order to successfully utilize thermoresponsive PNIPAm-*co*-PEGMa microgels for biomedical applications, one must optimize the PEGMa molecular weight and concentration in the copolymer in order to balance the temperature responsiveness with biocompatibility. Specifically, our results indicated that 20 wt.% of low molecular weight PEGMa (300 g/mol) incorporated in the copolymer can effectively suppresses the non-specific protein adsorption on these microgels, while giving a deswelling ratio that is only 18% less than that of PNIPAm microgels. Potential biomedical applications are protein or drug delivery systems, tissue engineering scaffolds as well as the development of anti-fouling coatings for biomedical implants.

Acknowledgements

Appendix A. Supplementary data

Supplementary data associated with this article can be found, in the online version, at http://dx.doi.org/10.1016/j.colsurfb.2012.10.053.

References

[1] H.G. Schild, Prog. Polym. Sci. 17 (1992) 163.
[2] (a) Y. Hirokawa, T. Tanaka, J. Chem. Phys. 81 (1984) 2;
    (b) S.T. Sun, I. Nishio, G. Swislow, T. Tanaka, J. Chem. Phys. 73 (1980) 5970.
[3] R.H. Pelton, H.M. Pelton, A. Morfesis, R.L. Rowell, Langmuir 5 (1989) 816.
[4] A. Hatefi, B. Amsden, J. Control. Release 80 (2002) 9.
[5] G.H. Hsiue, S.H. Hsub, C.C. Yang, Biomaterials 23 (2002) 6.
[6] G.H. Hsiue, S.H. Hsub, C.C. Yang, et al., Biomaterials 24 (2003) 8.
[7] H. Vihola, A. Laukkanen, L. Valtola, H. Tenhu, J. Hirvonen, Biomaterials 26 (2005) 3055.
[8] Y. Matsumaru, A. Hyodo, T. Nose, S. Ito, T. Hirano, S. Ohashi, J. Biomater. Sci. Polym. Ed. 7 (1996) 795.
[9] F.M. Veronese, G. Pasut, Drug Discovery Today 10 (2005) 1451.
[10] J.M. Harris, R.B. Chess, Nature Reviews Drug Discovery, vol. 2, 2003, p. 214.
[11] A. Gabizon, F. Martin, Drugs 54 (Suppl.) (1997) 15.
[12] F.M. Veronese, Biomaterials 22 (2001) 405.
[13] M. Diwan, T.G. Park, J. Control. Release 73 (2001) 233.
[14] K.D. Hinds, K.M. Campbell, K.M. Holland, D.H. Lewis, C.A. Piché, P.G. Schmidt, J. Control. Release 104 (2005) 447.
[15] S.M. Daly, T.M. Przybycien, R.D. Tilton, Langmuir 21 (2005) 1328.
[16] A. Abuchowski, T. van Es, N.C. Palczuk, F.F. Davis, J. Biol. Chem. 252 (1977) 3578.
[17] S. Sagnella, K. Mai-Ngam, Colloids Surf. B Biointer. 42 (2005) 147.
[18] D. Gan, L.A. Lyon, Macromolecules 35 (2002) 9634.
[19] J. Qin, Y.S. Jo, J.E. Ihm, D.K. Kim, M. Muhammed, Langmuir 21 (2005) 9346.
[20] H. Chen, L. Yuan, W. Song, Z. Wu, D. Li, Prog. Polym. Sci. 33 (2008) 1059.
[21] T. Trongsatitkul, B.M. Budhlall, Langmuir 27 (2011) 13468.
[22] N. Pardhy, B.M. Budhlall, Langmuir 26 (16) (2010) 13130–13141.
[23] R. Pelton, Adv. Colloid Interface Sci. 85 (2000) 1.
[24] R. Weissleder, Nat. Biotechnol. 19 (2001) 316–317.
[25] B.M. Budhlall, M. Marquez, O.D. Velev, Langmuir 24 (2008) 11959.
[26] N.J. Kruger, The bradford method for protein quantitation, in: A. Aitken, M. Learmonth (Eds.), The Protein Protocols Handbook, J.M. Walker Humana Press Inc., Totowa, NJ, 1996, p. 15.
[27] H.M. Crowther, B. Vincent, Colloid Polym. Sci. 276 (1998) 46.
[28] E. Daly, B.R. Saunders, Phys. Chem. Chem. Phys. 2 (2000) 3187.
[29] A. Guillermo, J.P. Cohen Addad, J.P. Bazile, D. Duracher, A. Elaissari, C. Pichot, J. Polym. Sci. B: Polym. Phys. 38 (2000) 889.
[30] W. McPhee, K.C. Tam, R.H. Pelton, J. Colloid Interface Sci. (1993) 156.
[31] C. Alava, B.R. Saunders, Colloids, A. Surfaces, Physicochem. Eng. Aspects 270–271 (2005) 18.
[32] J.A. Jones, N. Novo, K. Flagler, C.D. Pagnucco, S. Carew, C. Cheong, X.Z. Kong, N.A.D. Burke, H.D.H. Stöver, J. Polym. Sci. A: Polym. Chem. 43 (2005) 6095.
[33] K.H. Kim, J. Kim, W.H. Jo, Polymer 46 (2005) 2836.
[34] I.K. Kwon, T. Matsuda, Biomaterials 27 (2006) 986.
[35] C.M. Nolan, C.D. Reyes, J.D. Debord, A.J. Garcia, L.A. Lyon, Biomacromolecules 6 (2005) 2032.
[36] Y.-Z. You, D. Oupicky, Biomacromolecules 8 (2006) 98.
[37] C. Hong, M.A. Brook, C. Yang, H. Sheardown, J. Biomater. Sci. Polym. Ed. 16 (2005) 531.
[38] R.X. Zhuo, W. Li, J. Polym. Sci. Part A: Polym. Chem. 41 (2003) 152–159.
[39] T. Caykara, S. Kiper, G. Demirel, S. Semirci, C. Cakanyildrim, Polym. Int. 56 (2007) 275–282.
[40] T. Trongsatitkul, B. M. Budhlall, Polymer Chemistry, Accepted for publication November 2012.
[41] F.L. Gonza' lez Flecha, V. Levi, BAMBED 31 (5) (2003) 319–322.
[42] E.P.K. Currie, W. Norde, M.A. Cohen Stuart, Adv. Colloid Interface Sci. 100–102 (2003) 205.
[43] R.D. Waniska, J.K. Shetty, J.E. Kinsella, J. Agric. Food Chem. 29 (1981) 826–831.
[44] K.L. Prime, G.M. Whitesides, J. Am. Chem. Soc. 115 (1993) 10714–10721.
[45] P. Harder, M. Grunze, R. Dahint, G.M. Whitesides, P.E. Laibinis, J. Phys. Chem. B 102 (1998) 426–436.
[46] M. Skoda, R. Jacobs, J. Willis, F. Schreiber, Langmuir 23 (2007) 970–974.